

## CANARDS AND HORSESHOES IN THE FORCED VAN DER POL EQUATION

WARREN WECKESSER  
*Department of Mathematics*  
*Colgate University*  
*Hamilton, NY 13346*  
*E-mail: wweckesser@mail.colgate.edu*

Cartwright and Littlewood discovered “chaotic” solutions in the periodically forced van der Pol equation in the 1940’s. Subsequent work by Levinson, Levi, and others has made this singularly perturbed system one of the archetypical dissipative systems with chaotic dynamics. Despite the extensive history of this system, many questions concerning its bifurcations and chaotic dynamics remain. We use a combination of analysis of the singular limit and numerical simulation to describe a horseshoe map that arises in the three-dimensional phase space. The canards that form at a “folded saddle” play a crucial role in this analysis.

### 1. Introduction

We study the periodically forced van der Pol oscillator<sup>11</sup> in the form

$$\begin{aligned}\varepsilon \dot{x} &= y + x - \frac{x^3}{3}, \\ \dot{y} &= -x + a \sin(2\pi\theta), \\ \dot{\theta} &= \omega,\end{aligned}\tag{1}$$

where  $\theta \in \mathbb{R}/\mathbb{Z}$ , and  $0 < \varepsilon \ll 1$ . The goal of this report is to combine an understanding of the fast/slow dynamics of this singularly perturbed system with numerical studies to show the source of a horseshoe map in the three-dimensional phase space. The geometric picture presented here complements the analysis of Cartwright and Littlewood<sup>2,3,7,8</sup>.

By taking the limit  $\varepsilon = 0$  in (1) we obtain a differential-algebraic equation on the critical manifold  $C = \{(x, y, \theta) | y = x^3/3 - x\}$ . By eliminating  $y$  and then rescaling the vector field by  $x^2 - 1$ , we obtain the *slow flow*:

$$\theta' = \omega(x^2 - 1), \quad x' = -x + a \sin(2\pi\theta).\tag{2}$$

If we rescale time as  $\tau = \varepsilon t$  in (1), and then take the limit  $\varepsilon = 0$ , we

obtain the equation for the *fast dynamics*

$$x' = y + x - x^3/3, \quad (3)$$

where  $y$  is treated as a parameter, and the fast system is independent of  $\theta$ . Each point in the critical manifold  $C$  is an equilibrium point of (3). We decompose  $C$  into five subsets.  $C_s^+ = \{(x, y, \theta) \in C | x > 1\}$  and  $C_s^- = \{(x, y, \theta) \in C | x < -1\}$  are the subsets of  $C$  which are stable equilibria of the fast subsystem;  $C_u = \{(x, y, \theta) \in C | |x| < 1\}$  is the set of unstable equilibria of (3); the two lines  $S_{\pm 1} = \{(x, y, \theta) \in C | x = \pm 1\}$  are the fold lines.

When  $a > 1$ , the slow flow has equilibria at the points  $(\theta, x) = (\pm \sin^{-1}(1/a)/2\pi, \pm 1)$ . Two of these equilibria are saddle points. The other two equilibria are stable nodes if  $1 < a < \sqrt{1 + 1/(16\pi\omega)^2}$  and stable foci if  $a > \sqrt{1 + 1/(16\pi\omega)^2}$ . These equilibria are called folded equilibria because they lie on the fold curves of the critical manifold; they are not true equilibria of the van der Pol system (1). Let  $P_s$  be the saddle point on  $S_{-1}$ , let  $\gamma_s$  be the stable manifold of  $P_s$  in  $C_s^-$ , and let  $\gamma_c$  be the segment of the invariant manifold of  $P_s$  in  $C_u$  that is the smooth continuation of  $\gamma_s$  from  $P_s$  to the first intersection with  $S_{-1}$ . We phrase the definition this way because, while in the rescaled slow subsystem (2) this would be a stable manifold of  $P_s$ , we note that the direction of the flow of (2) on  $C_u$  is the reverse of the actual flow of (1). Trajectories of (1) close to  $\gamma_c$  flow *away* from the saddle, and  $\gamma_c$  acts like an unstable manifold. Finally,  $\theta_s$  is the  $\theta$  coordinate of the saddle on  $S_{-1}$ ,  $\theta_m$  is the  $\theta$  coordinate of the other end of  $\gamma_c$ , and  $\theta_u$  is the  $\theta$  coordinate of the first intersection with  $S_{-1}$  of the unstable manifold of  $P_s$  that lies in  $C_s^-$ . (See Figure 1.)

Figure 2 shows an example of a periodic orbit in the three dimensional phase space of (1). The vector field of the slow flow is shown in the surface  $C$ . The periodic orbit is a numerically computed solution to (1) with  $\varepsilon = 10^{-4}$ . As expected, the trajectory follows the slow flow when it is near  $C$ ; away from  $C$ , the trajectory is approximated by the fast subsystem.

## 2. The Folded Saddle and Canards

The behavior of trajectories near a folded saddle was analyzed by Benoit<sup>1</sup> (see also Mischenko, et al<sup>9</sup> and Szmolyan and Wechselberger<sup>10</sup>). We give an informal summary of the behavior. Consider a trajectory that is near the slow manifold  $C_s^-$ . The trajectory is approximated by the slow flow until it reaches a neighborhood of the fold. At a typical fold point, the trajectory makes a transition after which it is approximated by a segment

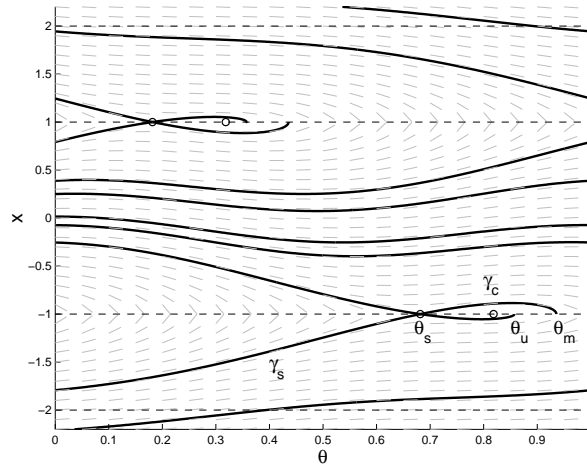


Figure 1. The phase portrait of the slow flow ( $a = 1.1$ ,  $\omega = 1.55$ ). The dashed lines at  $x = \pm 1$  are the fold lines, and the dashed lines at  $x = \pm 2$  are the projections of the fold lines in the fast direction. The small circles indicate equilibria.

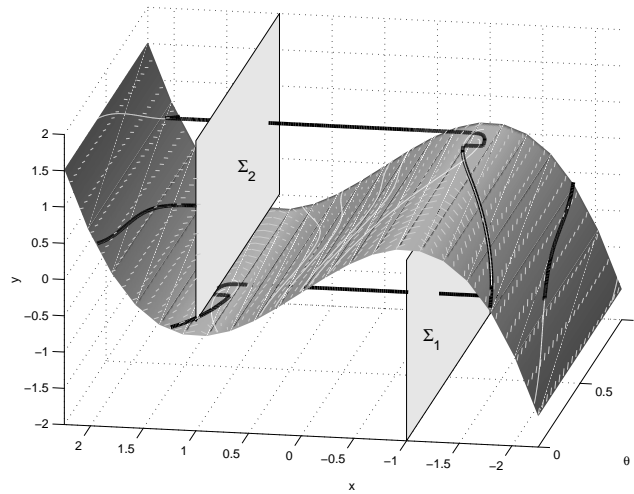


Figure 2. The gray surface is the critical manifold  $C$ . The white lines in  $C$  are the (numerically computed) invariant manifolds of the folded saddle in the slow flow. (These are the same curves plotted in black in Fig. 1.) The black curve is an unstable periodic orbit computed by AUTO, for the parameter values  $\varepsilon = 0.0001$ ,  $a \approx 1.1$ , and  $\omega = 1.55$ .

of the fast subsystem. Informally, we call this transition a “jump at the fold”. *Canards* may form near a folded saddle. These are trajectories that

do not jump at the fold, but instead remain close to the unstable sheet of the critical manifold after passing through a neighborhood of the fold. The slow segments of canards near the unstable sheet of the critical manifold will be close to  $\gamma_c$ . Since the trajectory is now near the unstable sheet of the slow manifold  $C_u$ , it will eventually diverge from  $C_u$  exponentially in the fast direction.

We classify the behavior of the canards by the direction in which they eventually jump off the unstable sheet. Those that jump back to the stable sheet where the trajectories began are the *jump-back* canards, and those that jump in the opposite direction (to land on a different sheet of the stable manifold) are the *jump-away* canards. The periodic orbit shown in Figure 2 contains an example of a jump-back canard. The initial conditions that give rise to the two types of canards are separated by an even smaller region in which a *maximal canard* forms. This is a canard that remains near the unstable manifold long enough to reach another fold. (In the full system, with  $\varepsilon > 0$ , there is not a unique maximal canard.) In this note we only consider an example where the maximal canard returns to the same fold as the one containing the folded saddle where the canard began.

### 3. The Poincaré Map

We define a Poincaré map  $\Phi$  for (1). Let  $\Sigma_1$  be the half cylinder  $\{(x, y, \theta) \mid x = -1, y < 2/3 - \delta\}$  for some small  $\delta > 0$  (see Figure 2), and let  $\Sigma_2 = \{(x, y, \theta) \mid x = 1, y > -2/3 + \delta\}$ . The system (1) is invariant under the symmetry transformation  $T(x, y, \theta) = (-x, -y, \theta + 1/2)$ , so rather than following the flow back to  $\Sigma_1$ , we use the symmetry  $T$  to map from  $\Sigma_2$  back to  $\Sigma_1$ . For  $\varepsilon$  sufficiently small, there is an open set of parameter values  $(a, \omega)$  such that the flow map from  $\Sigma_1$  to  $\Sigma_2$  composed with the symmetry transformation is a well defined map  $\Phi$  from  $\Sigma_1$  to itself.

Most trajectories beginning in  $\Sigma_1$  behave as follows. There is a fast jump to a neighborhood of the critical manifold, then a slow evolution (approximated by the slow flow (2)) to a neighborhood of the fold at  $x = -1$ , where the trajectory will jump to  $\Sigma_2$ . As explained above, canards form on trajectories sufficiently close to the stable manifold of the saddle. Let  $\kappa \subset \Sigma_1$  be the set of points for which canards will form during the flow from  $\Sigma_1$  to  $\Sigma_2$ . When these trajectories finally cross  $\Sigma_2$ , they have either jumped from a point near  $\gamma_c$  directly to  $\Sigma_2$  (the jump away canards), or they have jumped back to a neighborhood of  $C_s$  – and then jumped a second time, passing the fold between  $\theta_u$  and  $\theta_m$  (the jump back canards).

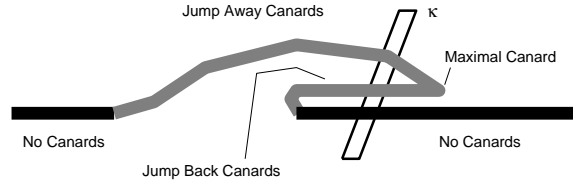


Figure 3. A qualitative sketch of the image of  $\Sigma_1$  under the Poincaré map  $\Phi$ . The union of the solid black and gray curves represents  $\Phi(\Sigma_1)$ . The white parallelogram represents a part of  $\kappa$ , and the gray segment represents  $\Phi(\kappa)$ .

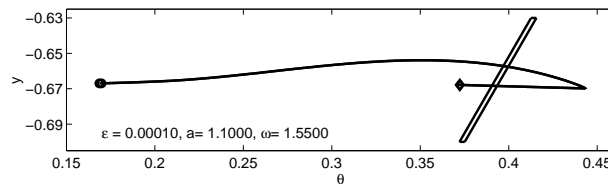


Figure 4. A Poincaré map that exhibits a horseshoe in (1). The parameter values are  $\varepsilon = 10^{-4}$ ,  $a = 1.1$  and  $\omega = 1.55$ .

For  $0 < \varepsilon \ll 1$ ,  $\kappa$  is a thin strip, given approximately by a thickened neighborhood of the set of points in  $\Sigma_1$  that project onto  $\gamma_s$ .

Because of the contraction onto the slow manifold, the image of  $\Sigma_1$  in  $\Sigma_2$  will be a thin strip. The image of  $\Sigma_1 \setminus \kappa$  in  $\Sigma_2$  will be a thin strip close to the line  $y = 2/3$ , with a gap from  $\theta_s$  to  $\theta_u$ . The ends of the gap are connected by the image of  $\kappa$ , which is also a thin strip that will be near the union of the projections onto  $\Sigma_2$  of  $\gamma_u$  and of the fold line between  $\theta_u$  and  $\theta_m$ . A qualitative sketch of the Poincaré map  $\Phi$  is shown in Figure 3. A horseshoe map is created when  $\Phi(\kappa)$  overlaps  $\kappa$ , as suggested in Figure 3.

To verify this qualitative picture for a specific set of parameter values, we used the program AUTO<sup>4</sup> as a boundary value problem solver to compute the Poincaré map when  $\varepsilon = 10^{-4}$ ,  $a = 1.1$  and  $\omega = 1.55$ . The result is shown in Figure 4. The curves in Figure 4 that end with the circles and diamonds are the images under the Poincaré map  $\Phi$  of the short horizontal line segments at the upper and lower ends of the thin parallelogram. The parallelogram was chosen to include a piece of the strip  $\kappa$ . The strong contraction on the stable slow manifold makes the resulting images indistinguishable in this plot. The combination of the contraction along the long direction of the parallelogram, the expansion along the horizontal direction (resulting from the formation of canards), and the fold that occurs at the

maximal canard are all the ingredients needed to show the existence of a horseshoe map with a hyperbolic invariant set.

### Acknowledgments

This work is part of an on-going collaboration<sup>5,6</sup> with John Guckenheimer of Cornell University and Kathleen Hoffman of the University of Maryland, Baltimore County. Some results presented in this paper were obtained during the summer of 2002 in a Research Experiences for Undergraduates Program at Cornell University sponsored by the National Science Foundation. Undergraduate participants in the forced van der Pol project were Katherine Bold, Chantal Edwards, Sabyasachi Guharay, Judith Hubbard, and Chris Lipa.

### References

1. É. Benoît. Canards et enlacements *Publ. Math. IHES Publ. Math.* **72**, 63–91 (1990).
2. M. Cartwright and J. Littlewood. On nonlinear differential equations of the second order: II the equation  $\ddot{y} - kf(y, \dot{y})\dot{y} + g(y, k) = p(t) = p_1(t) + kp_2(t)$ ,  $k > 0$ ,  $f(y) \geq 1$ . *Ann. Math.* **48**, 472–94 (1947).
3. M. Cartwright and J. Littlewood. Addendum to “On nonlinear differential equations of the second order: II,” *Ann. Math.* **50**, 504–505 (1949).
4. E. Doedel, R. Paffenroth, A. R. Champneys, T. F. Fairgrieve, Y. A. Kuznetsov, B. Sandstede, and X. Wang. *AUTO 2000: Continuation and Bifurcation Software for ODEs (with HomCont)* (2001).
5. J. Guckenheimer, K. Hoffman and W. Weckesser. The Forced van der Pol Equation I: The Slow Flow and its Bifurcations, *SIAM J. App. Dyn. Sys.*, **2**(1), 1–35 (2003).
6. K. Bold, C. Edwards, J. Guckenheimer, S. Guharay, K. Hoffman, J. Hubbard, R. Oliva, and W. Weckesser. The Forced van der Pol Equation II: Canards in the Reduced System, *SIAM J. App. Dyn. Sys.* (to appear).
7. J. Littlewood. On nonlinear differential equations of the second order: III the equation  $\ddot{y} - k(1 - y^2)\dot{y} + y = bk \cos(\lambda t + a)$  for large  $k$  and its generalizations. *Acta math.* **97**, 267–308 (1957).
8. J. Littlewood. On nonlinear differential equations of the second order: III the equation  $\ddot{y} - kf(y)\dot{y} + g(y) = bkp(\phi)$ ,  $\phi = t + a$  for large  $k$  and its generalizations. *Acta math.* **98**, 1–110 (1957).
9. E. Mischenko, Yu. Kolesov, A. Kolesov and N. Rozov. *Asymptotic methods in singularly perturbed systems* (Translated from the Russian by Irene Aleksanova. New York: Consultants Bureau), 1994.
10. P. Szmolyan and M. Wechselberger. Canards in  $R^3$ . *J. Diff. Eq.*, **177**, 419–453 (2001).
11. B. van der Pol. The nonlinear theory of electric oscillations *Proc. IRE* **22**, 1051-1086 (1934).